Nonnormality of Sonic Boom Loudness Metrics in the Turbulent Atmospheric Boundary Layer at Large Lateral Distances from the Flight Path

Alexander N. Carr[1*], Joel B. Lonzaga[1], and Steven A. E. Miller[2]

1. NASA Langley Research Center
2. University of Florida

* alexander.carr@nasa.gov

2pNS2
183rd Meeting of the Acoustical Society of America
December 6, 2022

Acknowledgements

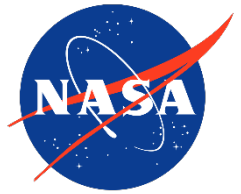

- This research was supported by the Commercial Supersonic Technology Project of the National Aeronautics and Space Administration under Grant No. 80NSSC19K1685.

- Thanks to Will Doebler, Alexandra Loubeau, Sriram Rallabhandi and others at the NASA Langley Structural Acoustics Branch for advice and guidance.

X-59 Flight Test Surveys

- Community response surveys to be conducted with X-59
  - Model dose-response relationship
  - Dose = sonic boom loudness metric (PL, ISBAP, A, B, D, E-SEL)
- Bayesian MLR approach to modeling dose response [1]
- Assumes no uncertainty in noise dose estimate
- Dose uncertainty included by Doebler et al. [2]
  - Estimated PL drawn from normal distribution
  - $\sigma_{dose\ uncertainty}$ estimated from measurements
    - WSPR2011: 3.7 dB
    - QSF18: 4.9 dB
- Turbulence effects are likely a big contributor to noise dose uncertainty

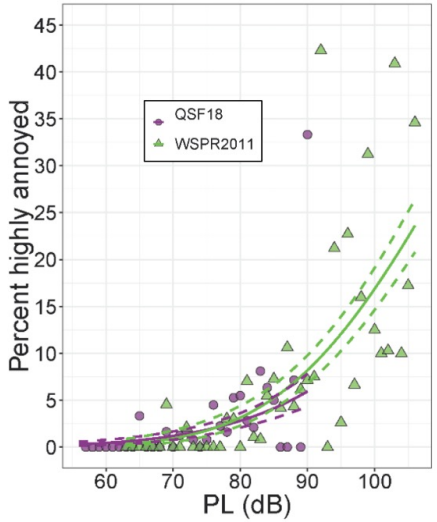

Dose-response relationship computed from BLMR for QSF18 and WSPR2011 [1]. Reproduced with permission [1]. Copyright 2020.

Artist's illustration of the NASA X-59 aircraft.

Turbulence Effects on Sonic Booms

- Atmospheric boundary layer (ABL) turbulence can cause variability in sonic boom waveforms [3,4,5]
- Dose variability may lead to flattening of dose-response curve
- Turbulence effects may be accounted for in simulations (see Refs. [6,7,8,9])
  - Computationally expensive
  - Quick estimates of $\sigma_{dose\ uncertainty}$ likely preferred

Calm Atmosphere

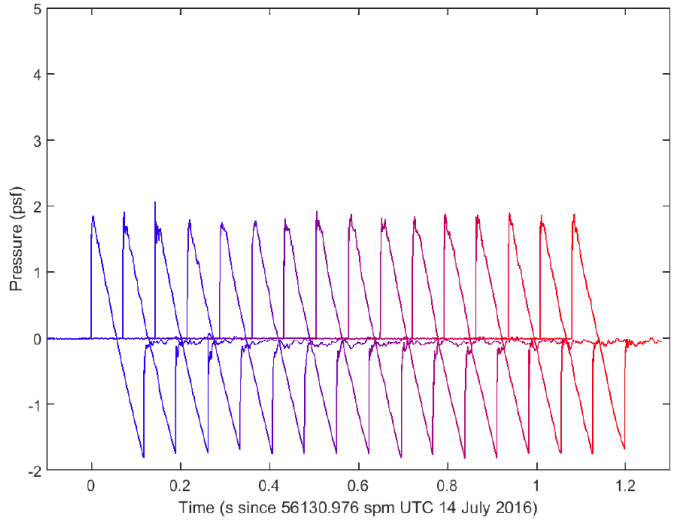

F-18 sonic boom measurements during SonicBAT at NASA AFRC in a calm atmosphere [4].

Turbulence Present

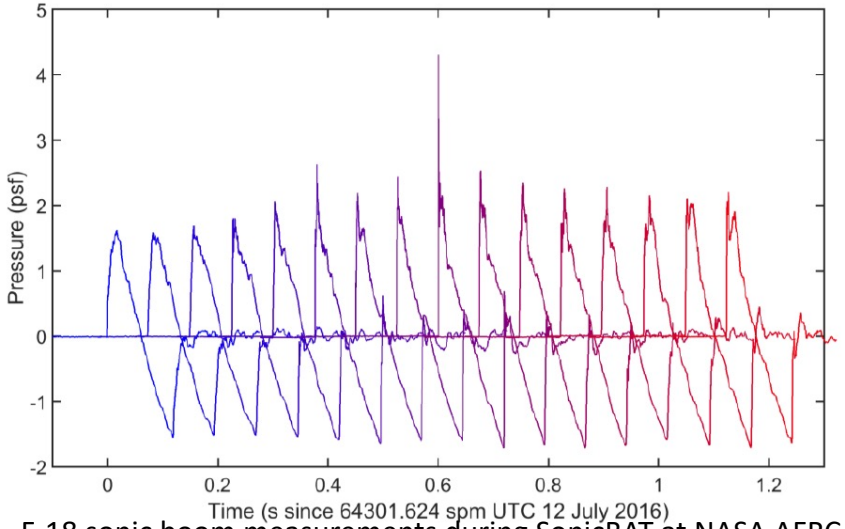

F-18 sonic boom measurements during SonicBAT at NASA AFRC in an atmosphere with turbulence present [4].

Objectives

Problems

- $\sigma_{dose\ uncertainty}$ will depend on turbulence conditions and propagation distance
- Dose uncertainty may not follow a normal distribution

Objectives

- Quantify dose uncertainty for N-waves and shaped booms (X-59)
- Examine normality of dose uncertainty

Method

- Past investigations simulate with KZK or FLHOWARD Eqns. (see Refs. [6,7,8,9])
- Present investigation: FLHOWARD type approach, but retain more terms

Outcome

- Approximate model of dose uncertainty based on simulation data
- Depends only on meteorological conditions, waveform, and metric

Simulation Approach

- Steps:
  1. Use PCBoom [11] to obtain input waveforms at z_i
  2. Simulate through computational domain with inhomogeneous ABL turbulence (using FLHOWARD-type equation, see Refs. [8,10])
  3. Compute $\sigma_{dose\ uncertainty}$ and sonic boom metric distributions along the propagation direction

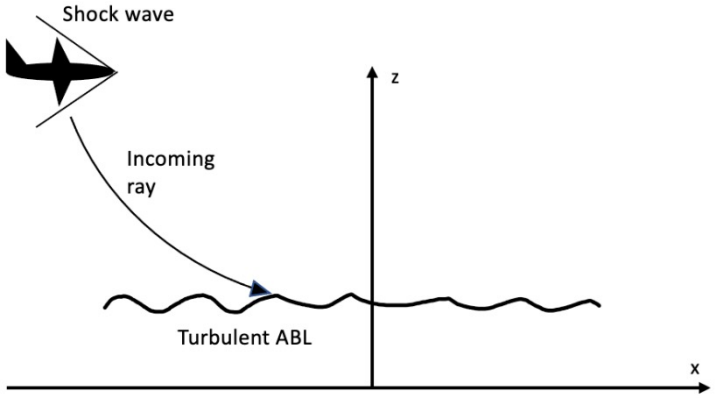

Diagram of ray propagation from source to ABL height.

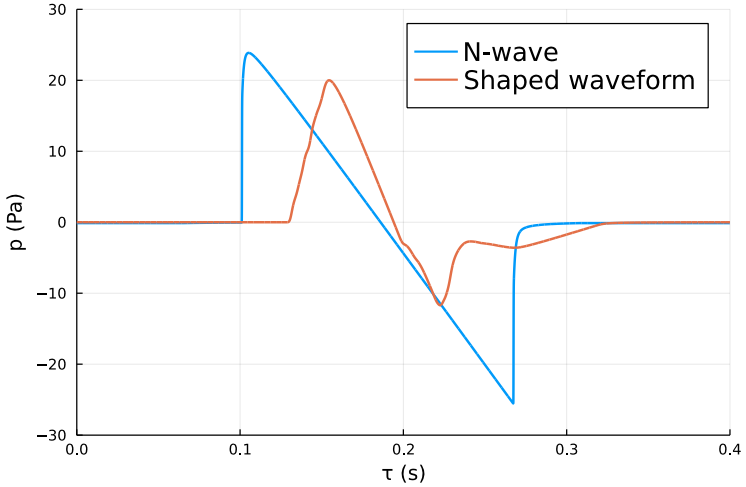

Initial waveforms at ABL height computed from PCBoom.

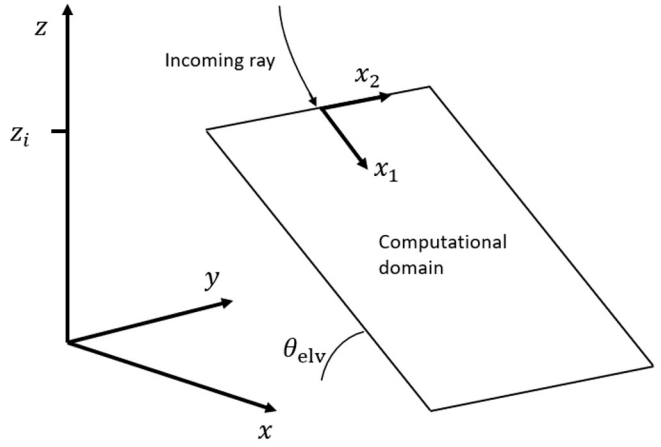

Computational domain of simulations.

Atmospheric Boundary Layer Conditions

- Convection level expresses relative importance of buoyancy effects to mean shear
- Will consider 3 different convection levels
  - Weak convection: $\log(-z_i L_o^{-1}) \leq 0.5$ (KSC)
  - Moderate convection: $0.5 < \log(-z_i L_o^{-1}) < 1.5$ (KSC)
  - Strong convection: $\log(-z_i L_o^{-1}) \geq 1.5$ (AFRC)
- Obukhov length, L_o, is a measure of production of TKE due to shear and buoyancy effects

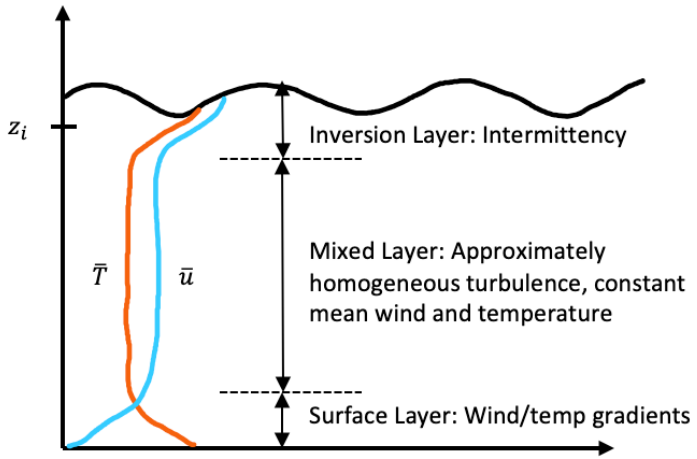

Illustration of daytime ABL.

Turbulence statistics in the mixed layer.

Flight No.	σ_T (K)	L_T (m)	σ_u (m/s)	L_u (m)	z_i (m)	$\log(-z_i L_o^{-1})$
KSC20	0.044	68.30	0.67	78.30	411.6	0.115
KSC1	0.086	71.20	0.78	89.20	457.3	0.451
KSC12	0.199	94.10	1.10	129.8	640.2	0.885
KSC6	0.406	65.20	1.11	96.70	457.3	1.342
KSC17	0.354	69.10	1.01	105.0	487.8	1.571
AFRC1	0.385	141.5	1.50	215.8	1000.0	1.601
AFRC2	0.341	189.4	1.52	297.4	1347.0	1.968
AFRC3	0.327	188.4	1.41	302.6	1344.0	2.459

Turbulence Generation

- Inhomogeneous: statistics vary with altitude
- Turbulence statistics model (Ostashev and Wilson [14])
- Temperature fluctuations

$$\frac{\sigma_T^2(z)}{T_*^2} = \frac{4}{(1-10\zeta)^{2/3}} \qquad \frac{L_T(z)}{z} = 2\frac{1-7\zeta}{1-10\zeta} \tag{1}$$

- Shear driven

$$\frac{\sigma_s^2}{u_*^2} = 3.0 \qquad \frac{L_s}{z} = 1.8 \tag{2}$$

- Bouyancy driven

$$\frac{\sigma_b^2}{w_*^2} = 0.35 \qquad \frac{L_b}{z_i} = 0.23 \tag{3}$$

- Turbulence generated with Generalized Random Phase Method (see Wilson [15])

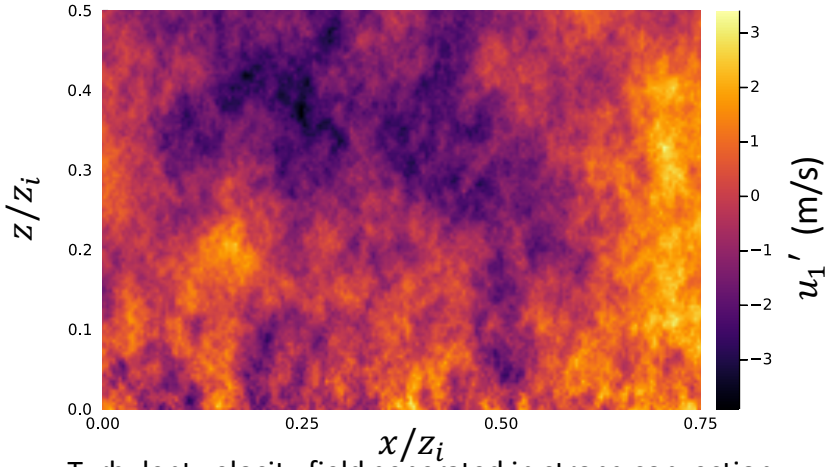

Turbulent velocity field generated in strong convection conditions.

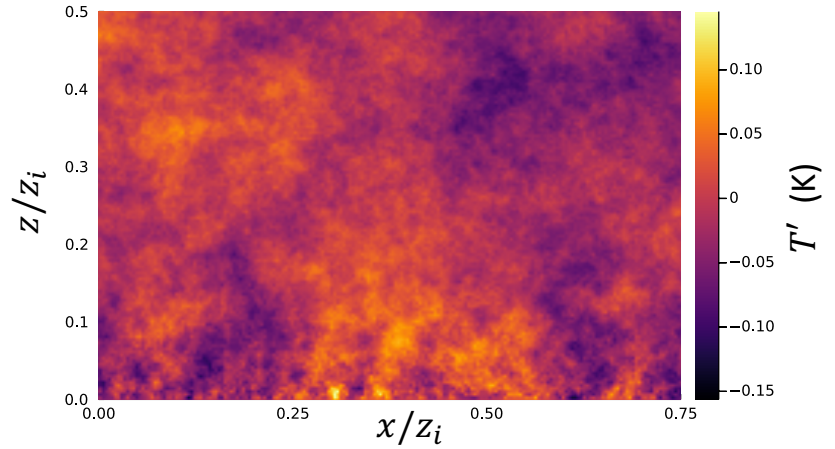

Turbulent temperature field generated in strong convection conditions.

Analogous Focal Length of Turbulence

- Index of refraction

$$n = 1 + \frac{u' + c'}{c_0} \tag{4}$$

- In the absence of humidity fluctuations, $c' c_0^{-1} = 0.5 T' T_0^{-1}$
- Effective focal length

$$\ell_f = \frac{C_1}{2} \mathcal{L} \frac{1 + \sigma_u c_0^{-1} + 0.5\, \sigma_T T_0^{-1}}{\sigma_u c_0^{-1} + 0.5\, \sigma_T T_0^{-1}} \tag{5}$$

- $\mathcal{L}/2$ is radius of curvature of equivalent "lens"
- Approximated as variance weighted average of L_T and L_u

$$\mathcal{L} = \frac{(\sigma_u c_0^{-1})^2 L_u + (0.5\, \sigma_T T_0^{-1})^2 L_T}{(\sigma_u c_0^{-1})^2 + (0.5\, \sigma_T T_0^{-1})^2} \tag{6}$$

- Empirical correction: $C_1 = 0.743 + 0.2087 \log(z_i)$

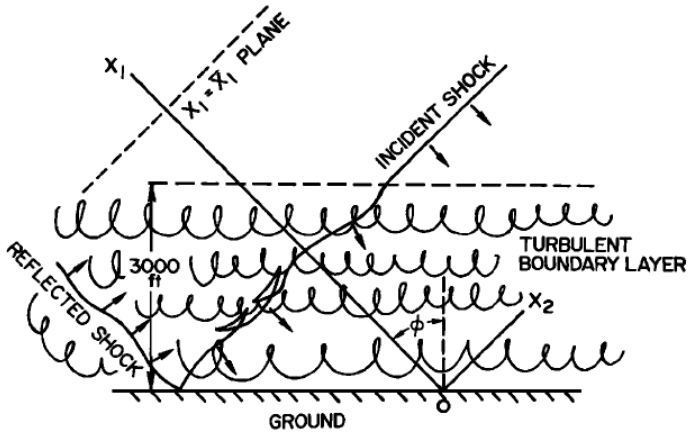

Illustration of turbulence effect on sonic boom wavefront. Reproduced with permission [16]. Copyright 1972.

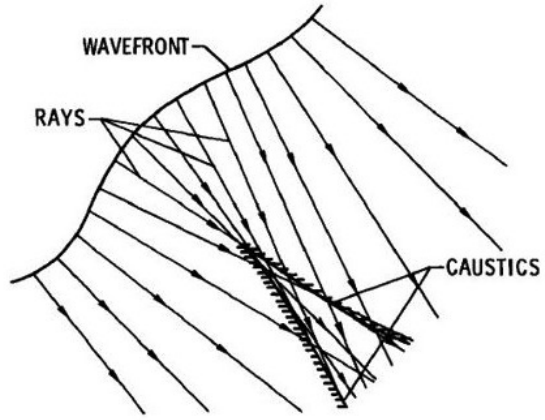

Illustration of caustic formation of a wavefront. Reproduced with permission [16]. Copyright 1972.

ℓ_f for each ABL setpoint.

	KSC20	KSC1	KSC12	KSC6	KSC17	AFRC1	AFRC2	AFRC3
ℓ_f	3890 m	3540 m	2948 m	2369 m	2763 m	2565 m	2724 m	3014 m

Dose Variability

- $\sigma_{\Delta \mathrm{PL}}$ standard deviation of Stevens Perceived level
- Maximum between 3 to 4 dB, similar to WSPR2011 and QSF18
- Linear increase for $x_1 \ell_f^{-1} \leq 0.5$

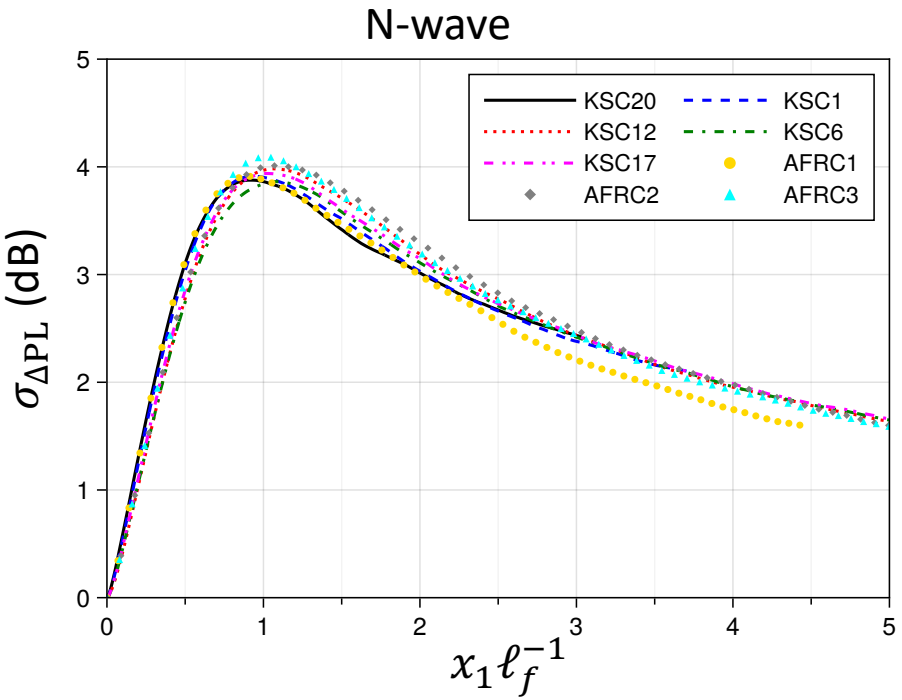

Standard deviation of PL for the sonic boom N-wave.

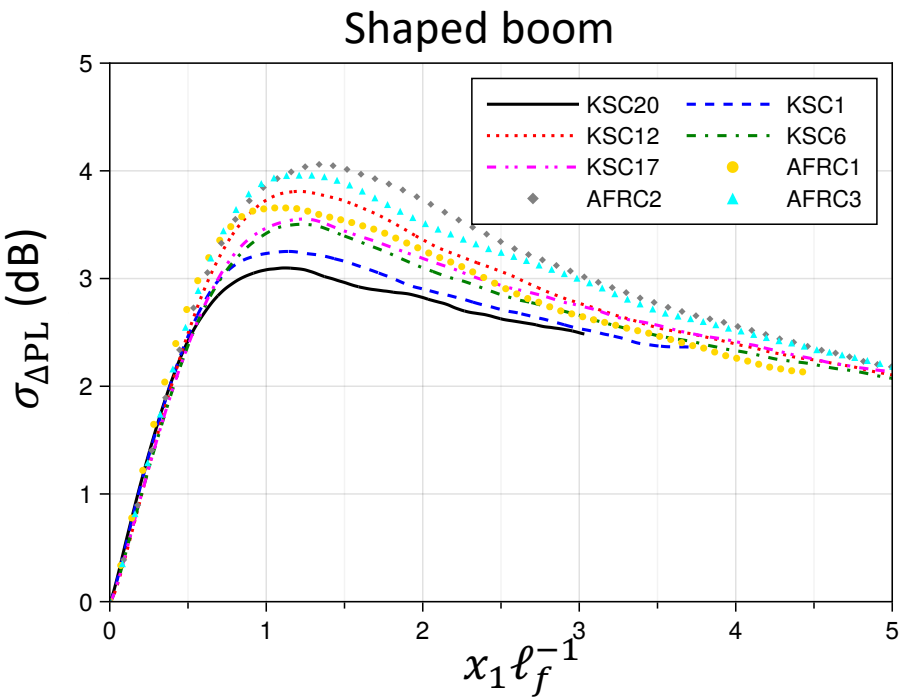

Standard deviation of PL for the shaped boom.

Probability Distributions

- PL distributions for strong convection
- Dashed line is normal distribution
- Less skewness present in shaped boom
- In general, skewness increases as
  - Lateral distance from flight track increases
  - Turbulence intensity and/or integral scale increases

Characteristics of the PL distributions relative to a normal distribution.

Range	Characteristics
$x_1 \ell_f^{-1} \leq 1$	Peaked/Skewed Left
$1 < x_1 \ell_f^{-1} < 3$	Normal/Slightly Peaked
$x_1 \ell_f^{-1} \geq 3$	Skewed Right

N-wave

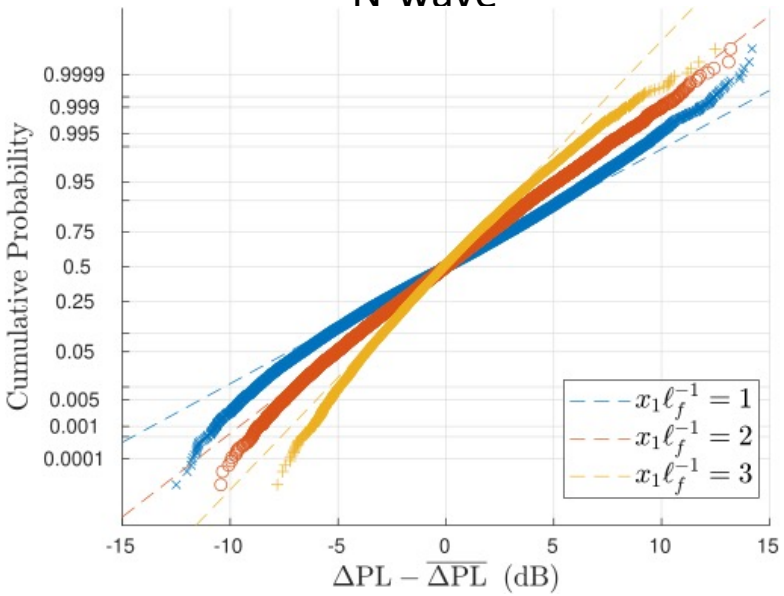

PL distributions at three non-dimensional propagation locations for the sonic boom N-wave in conditions of strong convection.

Shaped boom

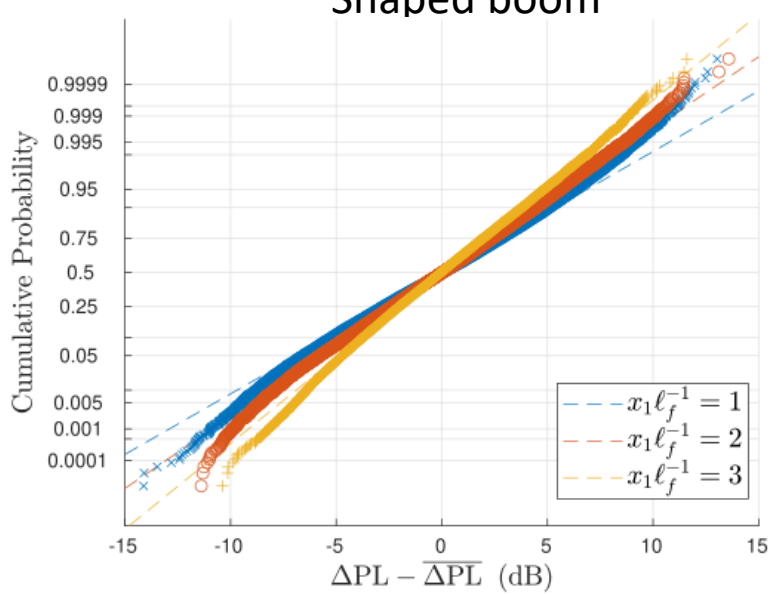

PL distributions at three non-dimensional propagation locations for the shaped boom in conditions of strong convection.

Approximate Model of PL Distribution

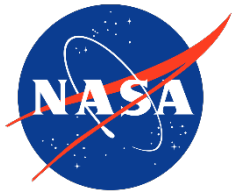

- Normal distribution appears to be a good approximation
- Dose uncertainty model

$$\sigma_{dose\ uncertainty} = \frac{A x_1 \ell_f^{-1}}{B + \left(x_1 \ell_f^{-1}\right)^{\alpha}} \tag{7}$$

- A, B, α are parameters determined by regression to simulation data
- Approximate dose uncertainty distribution

$$f(\Delta\mathrm{PL}) = \frac{1}{\sigma_{\Delta\mathrm{PL}}\sqrt{2\pi}} e^{-\frac{1}{2}\left(\frac{\Delta\mathrm{PL} - \mu_{\Delta\mathrm{PL}}}{\sigma_{\Delta\mathrm{PL}}}\right)^2} \tag{8}$$

Approximate Model of PL Distribution

- A, B, α can all be related to $\log(-z_i L_o^{-1})$
- Parameters for X-59 PL, according to regression

$$A \approx 6.32\, B$$
$$B \approx 0.94 + 0.25 \log(-z_i L_o^{-1})$$
$$\alpha \approx 1.68 + 0.94 \log(-z_i L_o^{-1})$$

- Will change depending on waveform and metric
- Model approximates $\sigma_{\Delta \mathrm{PL}}$ to within ± 0.25 dB
- Not valid beyond $x_1 \ell_f^{-1} > 5$

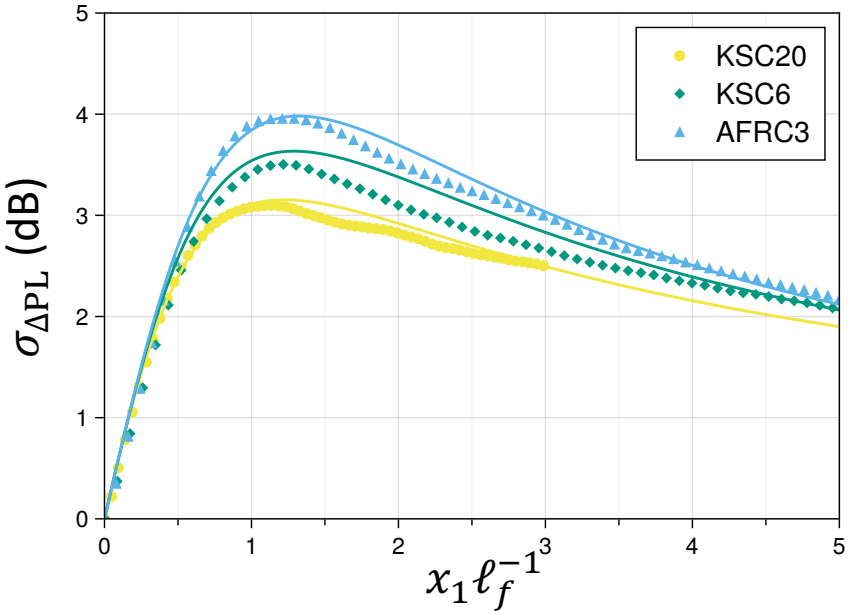

Model of $\sigma_{\Delta \mathrm{PL}}$ compared to simulation results for the shaped boom at three different ABL setpoints.

Comparison to Undertrack PL Simulations

- PDF approximates distributions observed both undertrack and off-track
- Does not capture skewness present in strong convection conditions and large lateral distances from flight path

Undertrack, Ground Level, AFRC3

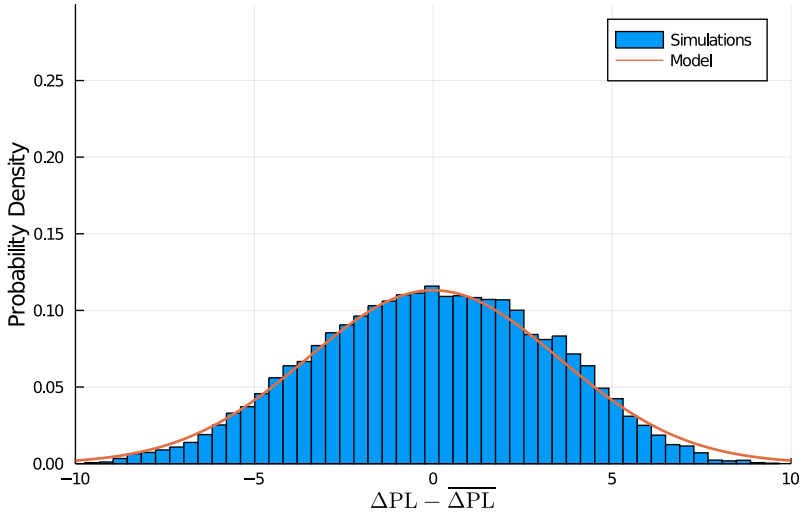

Probability density function model compared to simulation data at ground level for the shaped boom and ABL setpoint of AFRC3. Elevation angle of 35 degrees.

Off-track, Ground Level, AFRC3

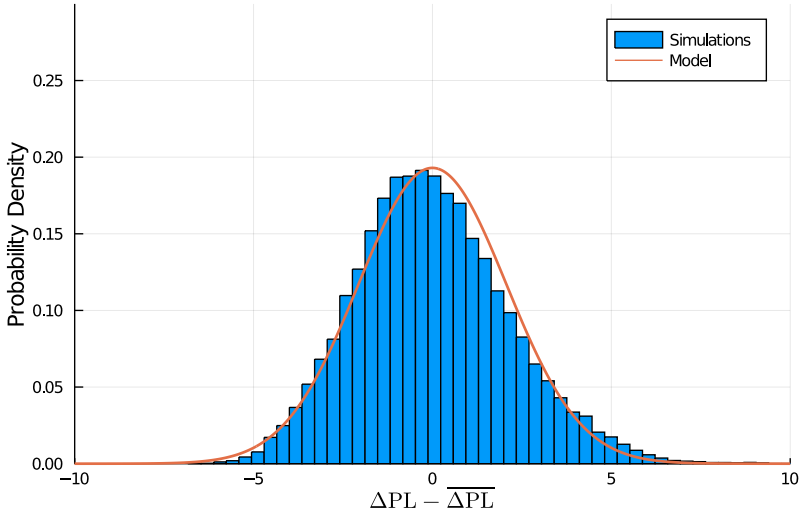

Probability density function model compared to simulation data at ground level for the shaped boom and ABL setpoint of AFRC3. Elevation angle of 5 degrees.

Summary

- Sonic boom simulations performed to estimate dose uncertainty due to turbulence
- Key outcomes
  - Parameter to collapse $\sigma_{\Delta \mathrm{PL}}$ for $x_1 \ell_f^{-1} \leq 0.5$
  - Model for dose uncertainty distributions
  - In some regions of the sonic boom carpet, normal distribution of dose uncertainty may not be appropriate
- Possible avenues forward
  - Use PCBoom in combination with meteorological data to estimate $x_1 \ell_f^{-1}$
  - Compare dose uncertainty model to measurements

Questions?

Thank you

References

1. J. Lee, J. Rathsam, and A. Wilson, “Bayesian statistical models for community annoyance survey data,” *The Journal of the Acoustical Society of America*, vol. 147, no. 4, pp. 2222–2234, Apr. 2020, doi: 10.1121/10.0001021.
2. W. Doebler, A. B. Vaughn, K. Ballard, and J. Rathsam, “The effect of modeling dose uncertainty on low-boom community noise dose-response curves,” *The Journal of the Acoustical Society of America*, vol. 150, no. 4, pp. A259–A259, Oct. 2021, doi: 10.1121/10.0008216.
3. H. H. Hubbard, D. J. Maglieri, V. Huckel, D. A. Hilton, Ground Measurements of Sonic-Boom Pressures for The Altitude Range of 10,000 to 75,000 Feet, Technical Report NASA-TR-R-198, NASA Langley Research Center, Hampton, Virginia, 1964.
4. D. J. Maglieri, T. L. Parrott, D. A. Hilton, W. L. Copeland, Lateral-Spread Sonic-Boom Ground-Pressure Measurements from Airplanes at Altitudes to 75,000 Feet and Mach Numbers to 2.0, Technical Report NASA-TN-D-2021, NASA Langley Research Center, Hampton, Virginia, 1963.
8. K. A. Bradley, C. M. Hobbs, C. B. Wilmer, V. W. Sparrow, T. A. Stout, J. M. Morgenstern, K. H. Underwood, D. J. Maglieri, R. A. Cowart, M. T. Collmar, H. Shen, P. Blanc-Benon, “Sonic booms in atmospheric turbulence (SonicBAT): The influence of turbulence on shaped sonic booms,” NASA Tech. Rep. NASA/CR-2020-220509, 2020.
1. T. Stout, Simulation of N-wave and shaped supersonic signature turbulent variations, Ph.D. dissertation, Pennsylvania State University, 2018.
2. F. Dagrau, M. Rénier, R. Marchiano, F. Coulouvrat, “Acoustic shock wave propagation in a heterogeneous medium: A numerical simulation beyond the parabolic approximation,” The Journal of the Acoustical Society of America, vol. 130, no. 20, pp. 20–32. Jul 2011. doi:10.1121/1.3583549.

References

8. D. Luquet, R. Marchiano, F. Coulouvrat, “Long range numerical simulation of acoustical shock waves in a 3d moving heterogeneous and absorbing medium,” Journal of Computational Physics, vol. 379, pp. 237–261, Feb 2019. doi:10.1016/j.jcp.2018.11.041.
9. A. N. Carr, J. B. Lonzaga, S. A. E. Miller, “Numerical prediction of loudness metrics for N-waves and shaped sonic booms in kinematic turbulence,” The Journal of the Acoustical Society of America, vol. 151, no. 6, pp. 3580–3593, Jun 2022. doi:10.1121/10.0011514.
10. A. N. Carr, Sonic Boom Propagation in the Turbulent Atmospheric Boundary Layer, Ph.D. dissertation, University of Florida, 2022.
11. K. J. Plotkin, M. Downing, J. Page, “USAF single event sonic boom prediction model: PCBOOM,” The Journal of the Acoustical Society of America, vol. 95, no. 5, pp. 2839–2839, May 1994. doi:10.1121/1.409605.
12. F. Coulouvrat, “New equations for nonlinear acoustics in a low Mach number and weakly heterogeneous atmosphere,” Wave Motion, vol. 49, no. 1, pp. 50–63, Jan 2012. doi:10.1016/j.wavemoti.2011.07.002
13. V.E. Ostashev, Acoustics in Moving Inhomogeneous Media, E & FN Spon, London, 1997.
14. V.E. Ostashev, D. K. Wilson, Acoustics in moving inhomogeneous media, CRC Press, Taylor & Francis Group, Boca Raton, FL, 2016.
15. D. K. Wilson, Turbulence Models and the Synthesis of Random Fields for Acoustic Wave Propagation Calculations., Technical Report ARL-TR-1677, Army Research Laboratory, Adelphi, MD, 1998.
16. A. D. Pierce and D. J. Maglieri, “Effects of atmospheric irregularities on sonic-boom propagation,” The Journal of the Acoustical Society of America, vol. 51, no. 2C, pp. 702–721, Feb. 1972. [Online]. Available: https://doi.org/10.1121/1.1912904

Extra Slides

Abstract

- Atmospheric boundary layer (ABL) turbulence causes variability of the sonic boom waveform at the ground. Recent numerical investigations of sonic boom propagation through kinematic velocity fluctuations indicate that loudness metric distributions are positively skewed relative to a normal distribution. This skewness depends on the propagation distance and turbulence intensity. Propagation simulations of N-waves and shaped booms through inhomogeneous ABL turbulence are presented. Meteorological conditions are varied to examine different daytime ABL conditions and their effect on sonic boom loudness distributions. Two outcomes are observed: 1) the loudness metric distributions become increasingly positively skewed as the propagation distance through the ABL increases, and 2) the distributions become increasingly positively skewed at the same lateral distance from the flight path as the convection level of the daytime ABL is increased. Thus, results indicate that ground level measurements of sonic boom loudness from flight tests performed at large lateral distances from the flight path may not be normally distributed, due to turbulence present in the ABL. (This research is supported by the Commercial Supersonic Technology Project of the National Aeronautics and Space Administration under Grant No. 80NSSC19K1685.)

Numerical Method

- Coulouvrat [12] and Ostashev [13]

$$\frac{1}{\breve{c}^2}\frac{\breve{D}^2 p}{\breve{D}t^2} - \breve{\rho}\frac{\partial}{\partial x_i}\left(\frac{1}{\breve{\rho}}\frac{\partial p}{\partial x_i}\right) = -2\frac{\partial \breve{u}_j}{\partial x_i}\int_{-\infty}^{t}\frac{\partial^2 p}{\partial x_i \partial x_j}dt' + \frac{\delta}{\breve{c}^4}\frac{\partial^3 p}{\partial t^3} + \frac{\beta}{\breve{\rho}\breve{c}^4}\frac{\partial^2 p^2}{\partial t^2}$$

- Partially one-way equation

$$\frac{\partial^2 p}{\partial x_1 \partial \tau} = \mathcal{D}(p) + \mathcal{H}(p) + \mathcal{N}(p) + \mathcal{A}(p)$$

- Integrate forward in x_1 with split-step method

$$p(x_1 + \Delta x_1, x_2, \tau) = p^{\mathcal{N}}_{\Delta x_1/2} p^{\mathcal{H}+\mathcal{A}}_{\Delta x_1/2} p^{\mathcal{D}}_{\Delta x_1} p^{\mathcal{H}+\mathcal{A}}_{\Delta x_1/2}\, p^{\mathcal{N}}_{\Delta x_1/2}$$

- Parabolic approximation only on $\mathcal{H}$

Numerical Method

- Diffraction: Angular spectrum method
  - Accurate at all forward angles
- Heterogeneities: Two methods
  - Exact solution of ODE involving terms with x_1 and τ derivatives
  - Crank-Nicolson integration of remaining terms
- Nonlinearities: Burgers-Hayes algorithm
- Atmospheric absorption: Compute attenuation assuming no dispersion
- Validated with benchmark problems
- Agreement within 2% of analytical solutions

Angular Spectrum Method

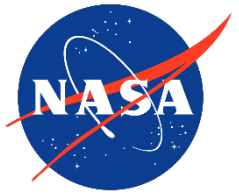

- Helmholtz Eqn. in delayed time

$$\frac{2i\omega}{c_0}\frac{\partial \hat{p}}{\partial x_1} = \frac{\partial^2 \hat{p}}{\partial x_1^2} + \frac{\partial^2 \hat{p}}{\partial x_2^2}$$

- Take cosine transform in x_2 (sound hard boundary)
- Finite impedance boundaries
  - Combination of cosine and sine transform
  - Not considered here
- Angular spectrum, $A(x_1, k_2, \omega) = \int_0^\infty \hat{p}(x_1, x_2, \omega)\cos(k_2 x_2)dx_2$
- Evolution governed by,

$$\frac{d^2A}{dx_1^2} - \frac{2i\omega}{c_0}\frac{dA}{dx_1} - k_2^2 A = 0$$

Generalized Random Phase Method

- Consider POD [15]

$$\int \hat{R}_{ij}(k_x, z, z')\phi_j^{(m)}(k_x, z')dz' = \lambda^{(n)}(k_x)\phi_i^{(n)}(k_x, z)$$

- Use eigenvalues to construct turbulent field

$$\hat{u}_i'(k_x, z) = \sum_{n=1}^{N} \lambda^{(n)}(k_x)\phi_i^{(n)}(k_x, z)$$

- Inverse F.T. to obtain $u_i'(x, z)$
- von Karman model for $\hat{R}_{ij}(k_x, z, z')$ [16,17]
- $\sigma_u^2 = \sigma_b^2 + \sigma_s^2$
- $L_u = \left(\sigma_b^2 L_b + \sigma_s^2 L_s\right)/\sigma_u^2$

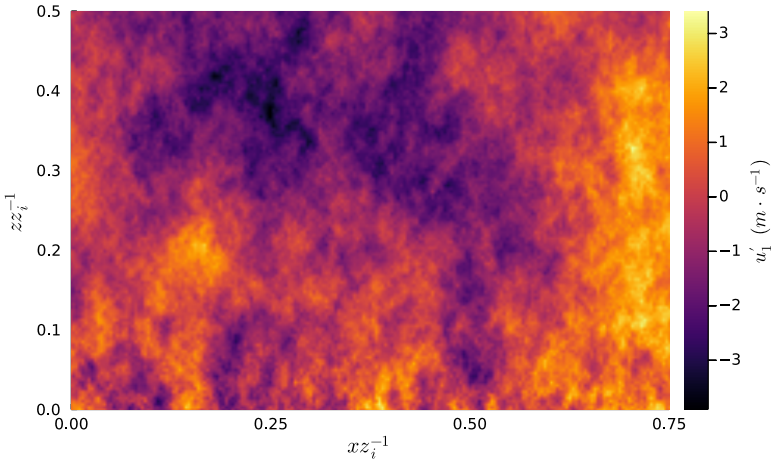

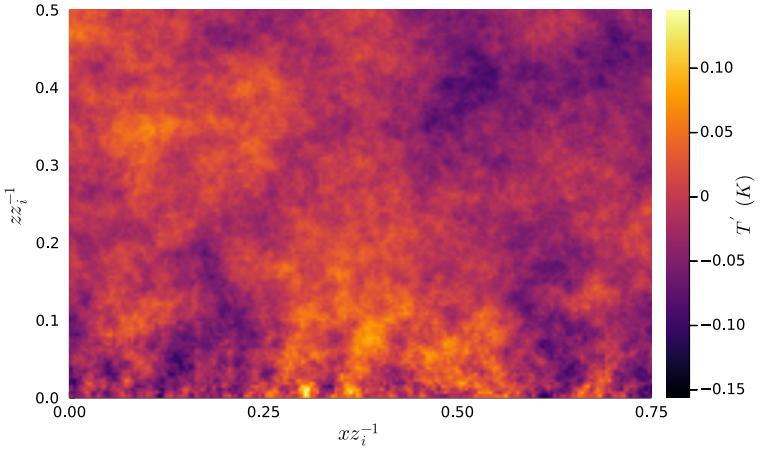

Analogous Focal Length of Turbulence

- Unable to collapse caustic PDFs
- Correction to ℓ_f for increasing integral scales
- Let C_1 be a function of z_i

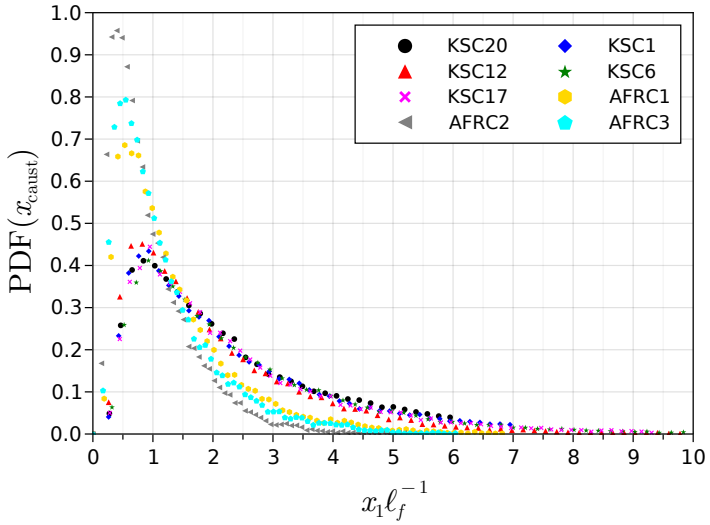

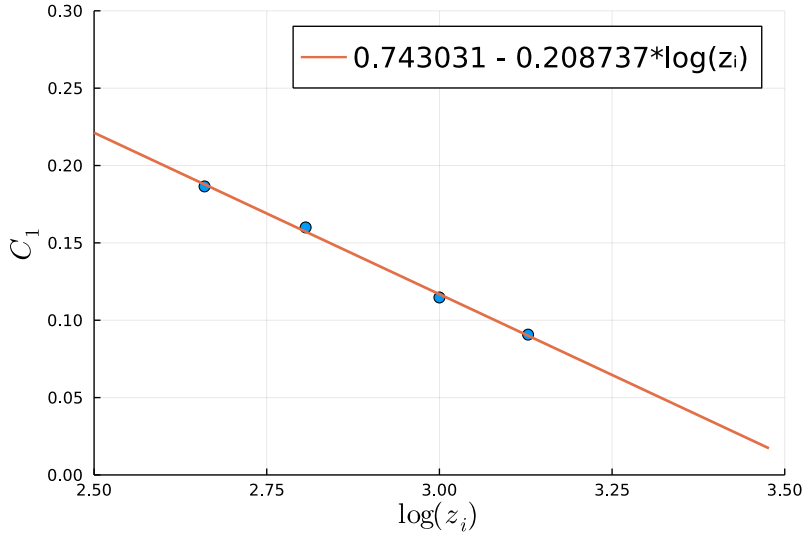

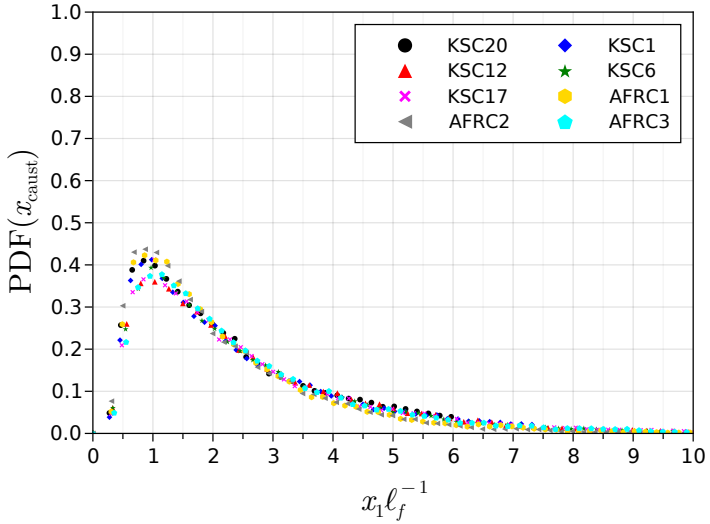

ISBAP Variability

- ISBAP standard deviation

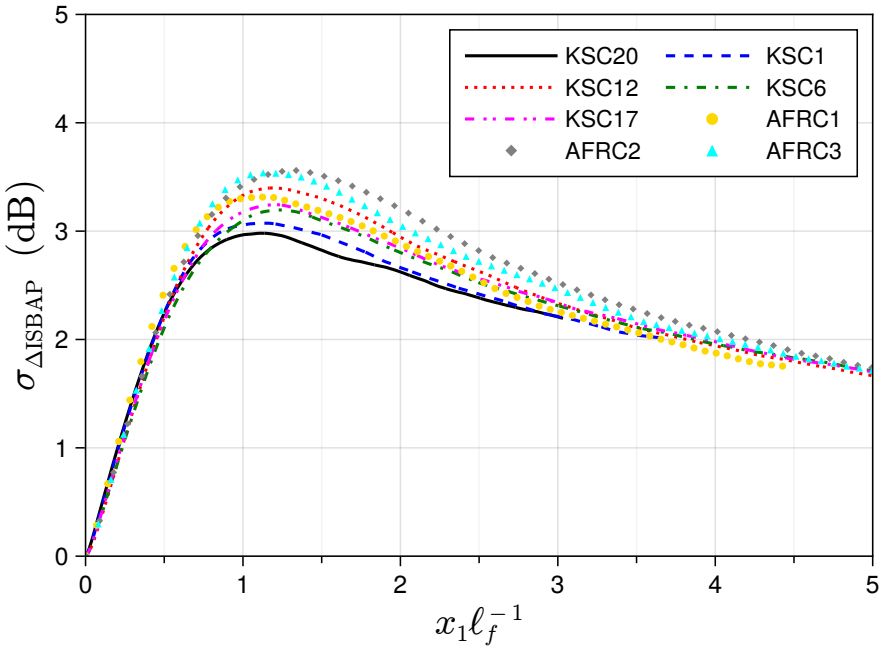

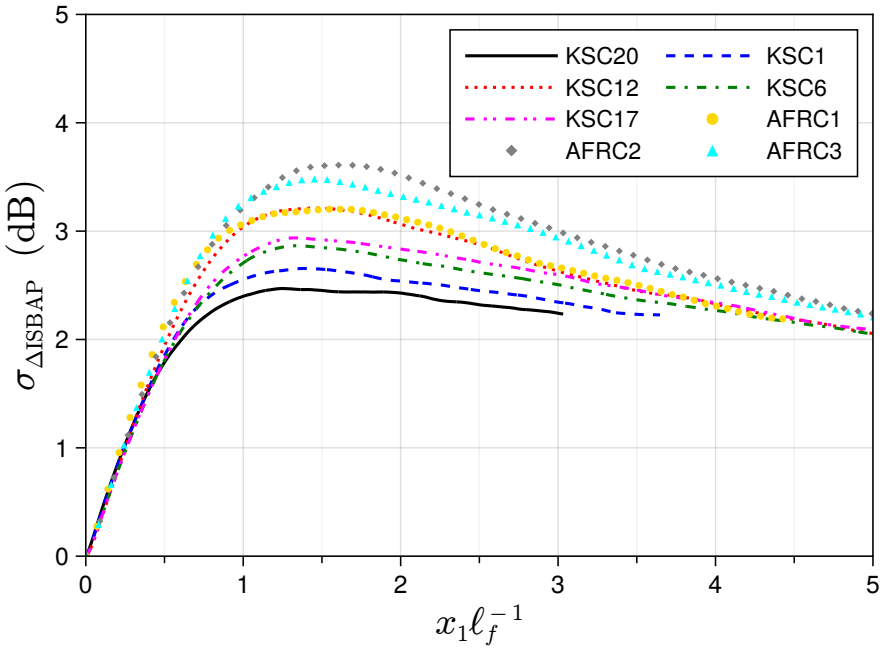

BSEL Variability

- BSEL standard deviation

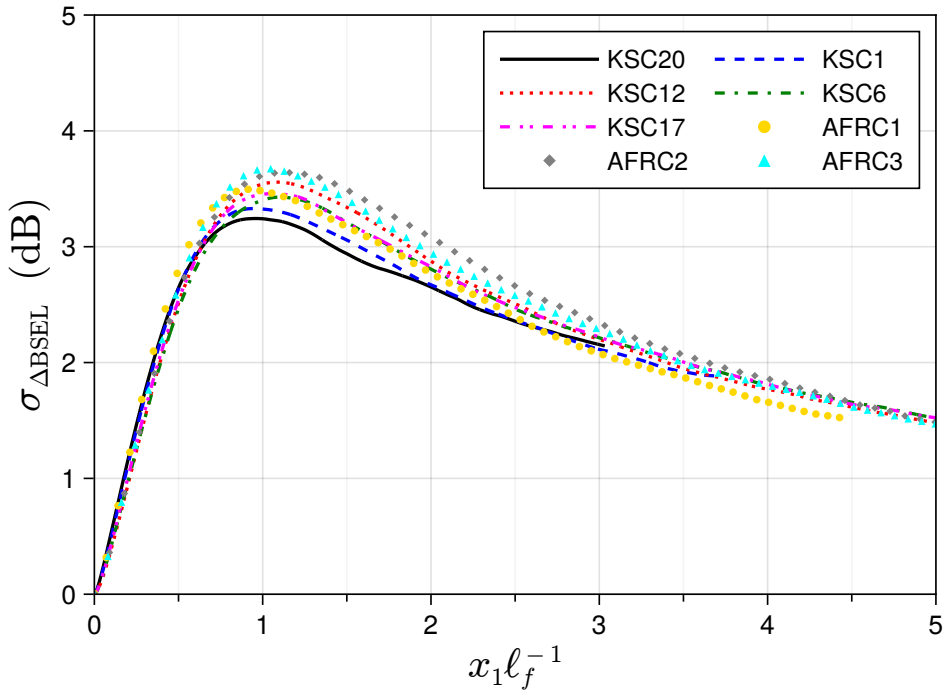

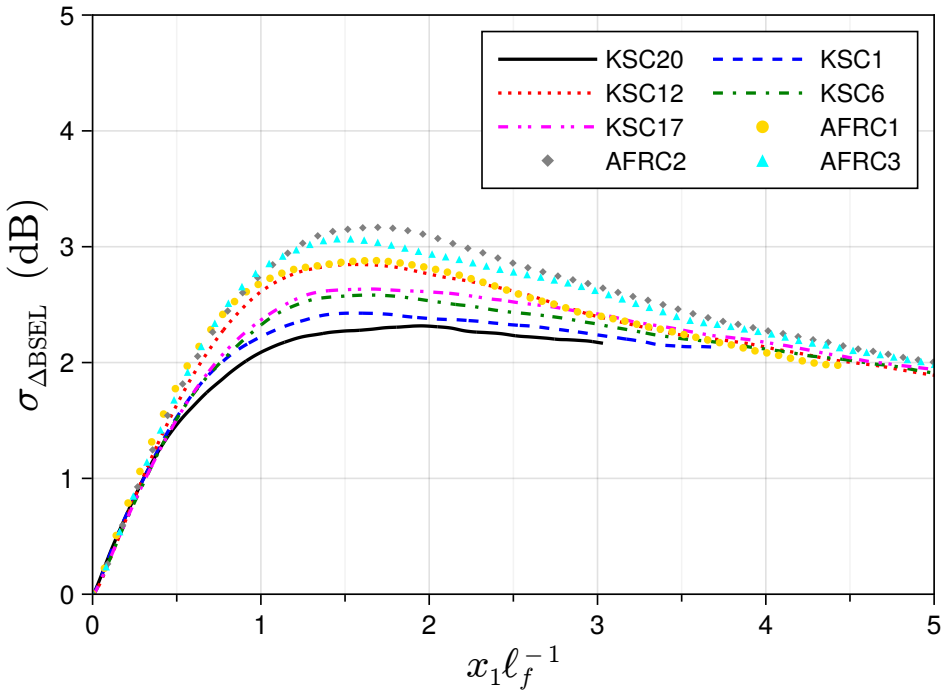

ISBAP Distribution

- ISBAP distributions for strong convection

N-wave

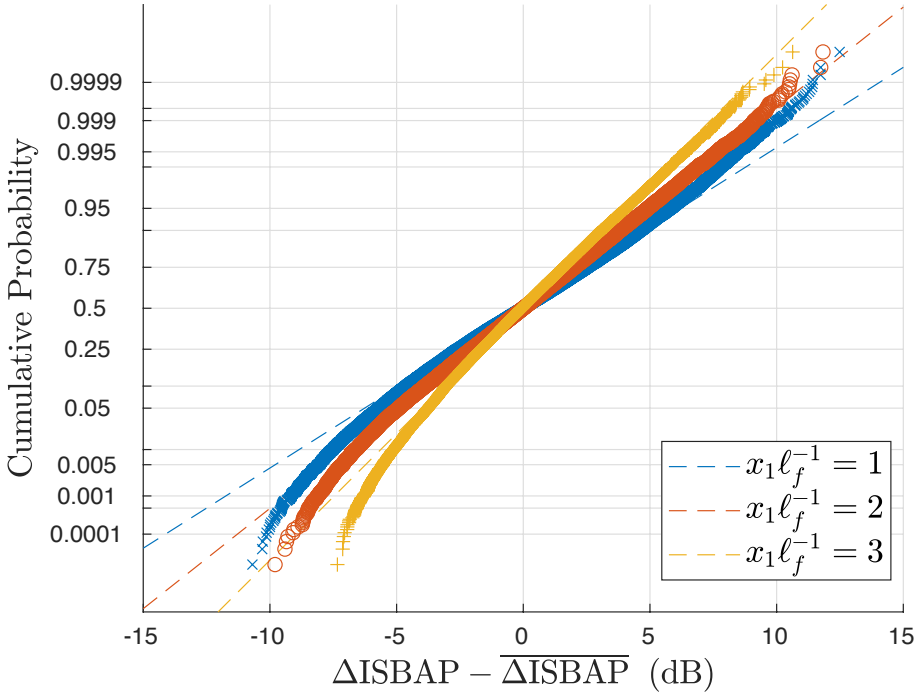

Shaped boom

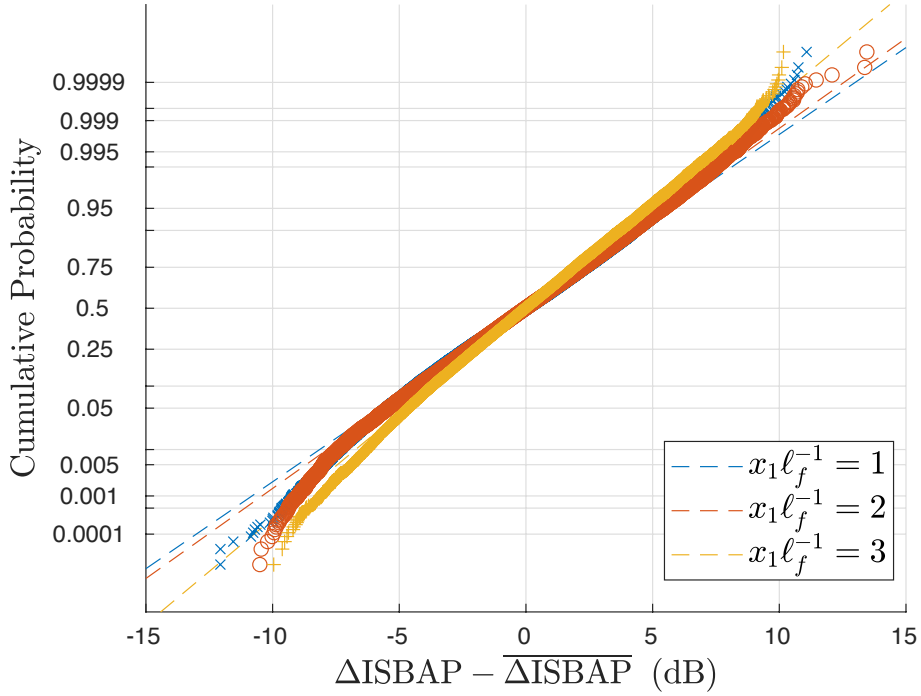

BSEL Distribution

- BSEL distributions for strong convection

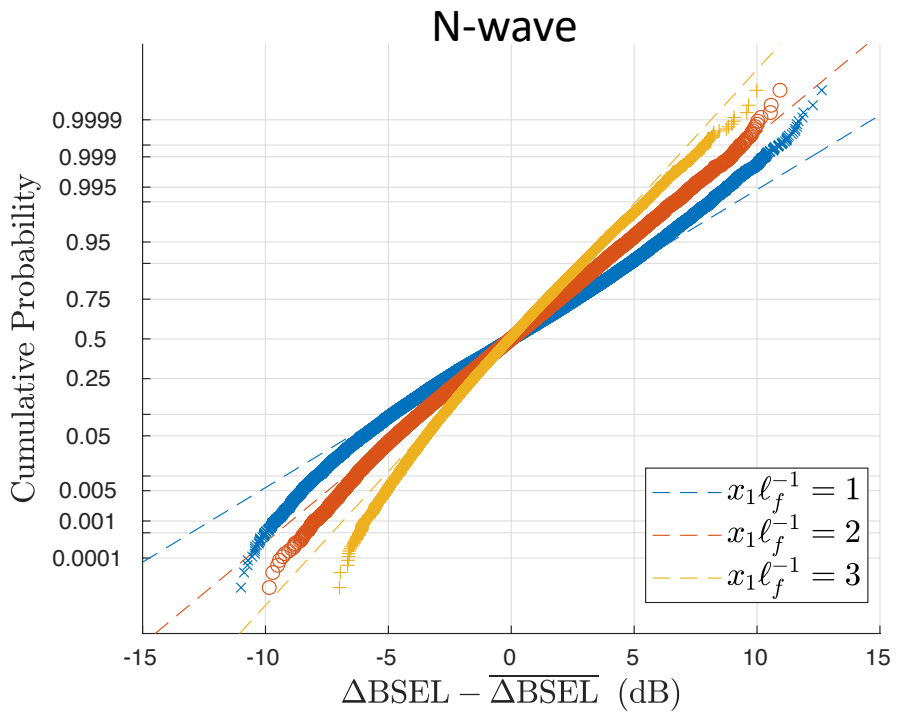

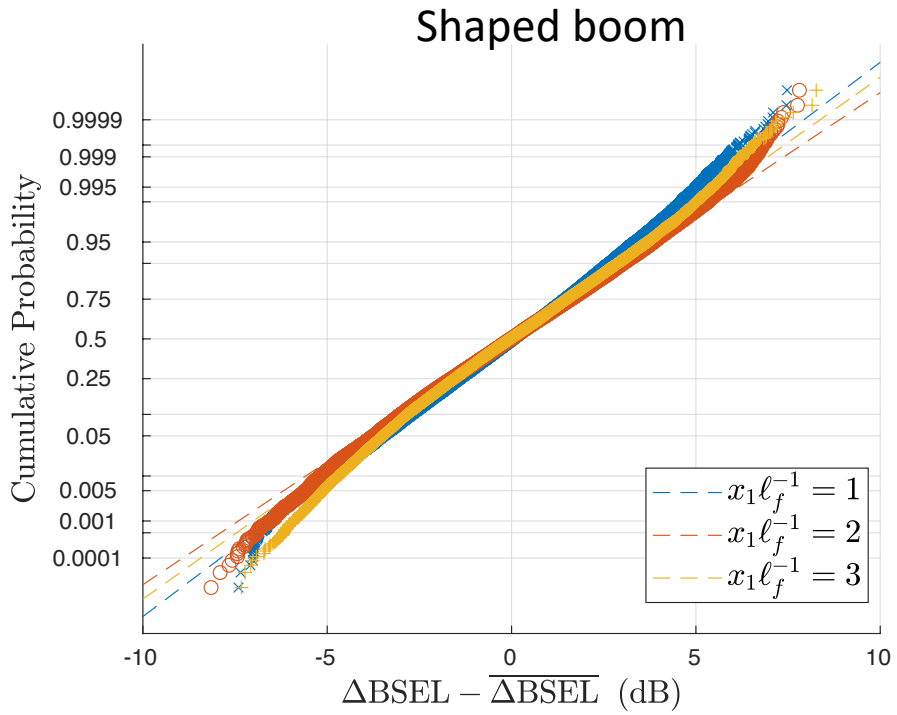

Regression Parameters

- α and B are functions of the convective parameter

$$\alpha, B \approx C_1 + C_2 \log(-z_i L_o^{-1})$$

- A/B should be constant, since in the limit $x_1 \ell_f^{-1} \to 0$ the slope is the same for all cases

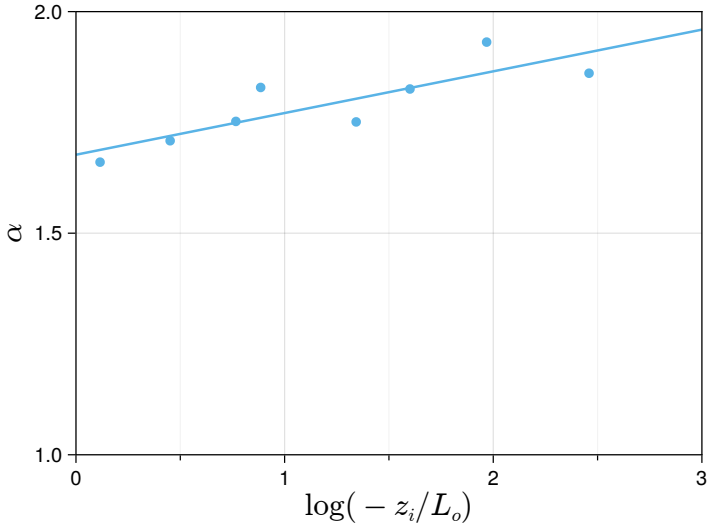

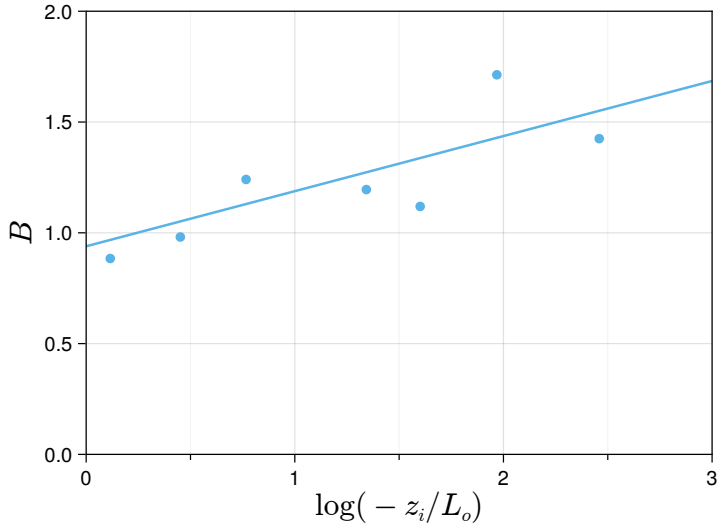

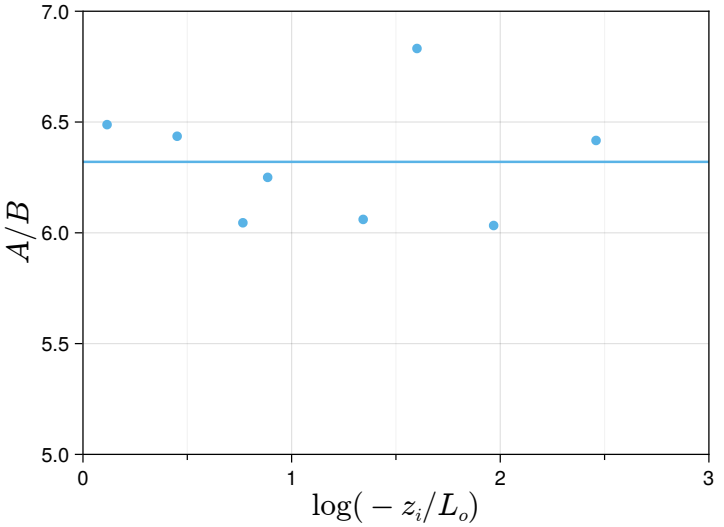

KSC20 Model Distribution Comparison

- KSC20 simulations compared to model PDF

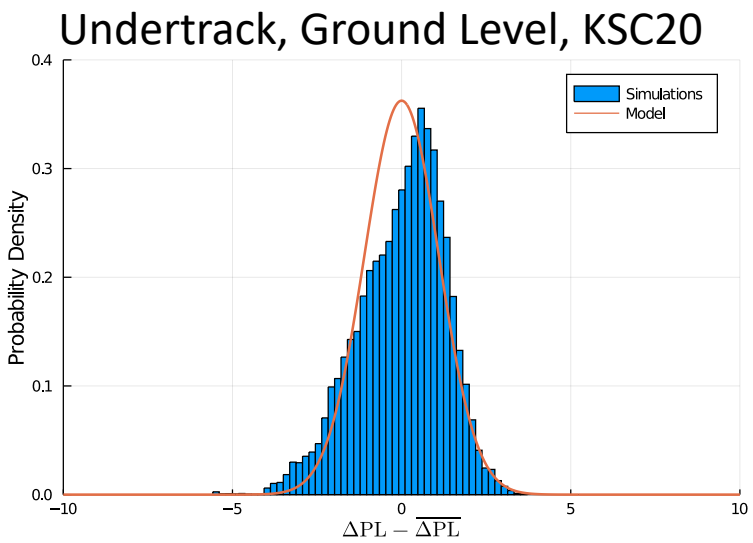

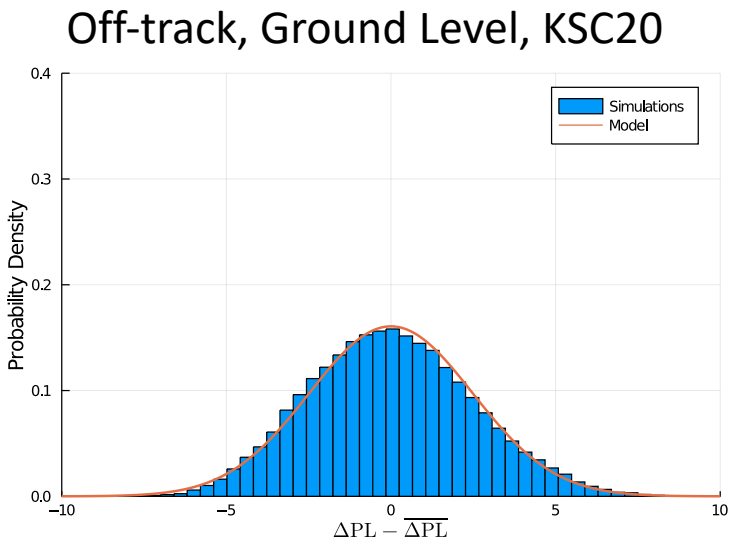

KSC6 Model Distribution Comparison

- KSC6 simulations compared to model PDF